Healing of Incisional Wounds in the Embryonic Chick Wing Bud: Characterization of the Actin Purse-String and Demonstration of a Requirement for Rho Activation

Jane Brock,* Katie Midwinter,‡ Julian Lewis,§ and Paul Martin*

*Department of Anatomy & Developmental Biology and Department of Plastic Surgery, University College London, London WC1E 6BT, United Kingdom; ‡Department of Human Anatomy, University of Oxford, Oxford OX1 3QX, United Kingdom; and §Imperial Cancer Research Fund Developmental Biology Unit, Department of Zoology, University of Oxford, Oxford OX1 3PS, United Kingdom

Abstract. Small skin wounds in the chick embryo do not heal by lamellipodial crawling of cells at the wound edge as a skin wound does in the adult, but rather by contraction of an actin purse-string that rapidly assembles in the front row of epidermal cells (Martin, P., and J. Lewis. 1992. *Nature (Lond.).* 360:179–183). To observe the early time course of actin purse-string assembly and to characterize other cytoskeletal components of the contractile machinery, we have followed the healing of incisional or slash wounds on the dorsum of the chick wing; these wounds take only seconds to create and heal within ~6 h. Healing of the epithelium depends on a combination of purse-string contraction and zipper-like closure of the gap between the cut edges of the epithelium. Confocal laser scanning microscope studies show that actin initially aligns into a cable at the wound margin in the basal layer of the epidermis within ~2 min of wounding. Coincident with actin cable assembly, we see localization of cadherins into clusters at the wound margin, presumably marking the sites where segments of the cable in adjacent cells are linked via adherens junctions. A few minutes later we also see localization of myosin II at the wound margin, as expected if myosin is being recruited into the cable to generate a contractile force for wound healing. At the time of wounding, cells at the wound edge become transiently leaky, allowing us to load them with reagents that block the function of two small GTPases, Rho and Rac, which recently have been shown to play key roles in reorganiztion of the actin cytoskeleton in tissue-culture cells (Hall, A. 1994. *Annu. Rev. Cell Biol.* 10:31–54). Loading wound edge epidermal cells with C3 transferase, a bacterial exoenzyme that inactivates endogenous Rho, prevents assembly of an actin cable and causes a failure of healing. No such effects are seen with N17rac, a dominant inhibitory mutant Rac protein. These findings support the view that in this system the actin cable is required for healing—both the purse-string contraction and the zipping up—and that Rho is required for formation of the actin cable.

THE self-sealing behavior of the epidermis in embryonic wounds provides a simple model in which to examine some of the basic general principles of epithelial movement and cohesion during development. In a previous study of embryonic wound healing, we examined the migratory capacity of the embryonic epidermis by making excisional skin wounds in limb-bud stage chick embryos (Martin and Lewis, 1992). At this stage the embryonic skin consists simply of a bilayered epidermis beneath which is a rather loose homogeneous mesenchyme, not yet differentiated into dermis. By marking the initially exposed mesenchyme with a lipophilic marker dye, DiI, we showed that wounded epidermis swept in over the mesenchyme (which itself meanwhile contracted) (McCluskey and Martin, 1995), but at no stage during the healing process did we observe lamellipodia at the epidermal wound front. Rather, it seemed as though the epidermal cells were drawn forward by a circumferential tension exerted around the margin of the wound, acting like a purse-string to pull the wound edges together. Thus, while the cells at the leading edge of an adult lesion move forward by anchoring to the substratum and crawling over it (Odland and Ross, 1968; Buck, 1979; for reviews see Stenn and DePalma, 1988; Grinnell, 1992), the leading cells of an embryonic wound appear to be drawn forward simply by concerted tugging on their epithelial cell neighbors. Correspondingly, we found a cable of actin running in the front row of basal epidermal cells at the margin of the embryonic wound (Martin and Lewis, 1992). A subsequent paper showed that the same was true of a gut epithelial cell line wounded as a confluent monolayer (Bement et al., 1993).

Address all correspondence to Paul Martin, Departments of Anatomy & Developmental Biology and Plastic Surgery, University College London, Gower Street, London WC1E 6BT, United Kingdom. Tel.: (44) 171-419-3362. Fax: (44) 171-380-7349. e-mail: paul.martin@ucl.ac.uk

These authors also showed localization of myosin II to the actin purse-string, providing evidence for the presence of contractile motors necessary for the epithelial movement. We have recently shown that preventing formation of the actin cable at the margin of embryonic wounds by culturing in the presence of cytochalasin D completely inhibits reepithelialization of the wound (McCluskey and Martin, 1995).

A similar involvement of actin and myosin in epithelial closure movements has been demonstrated in a different way by Young and colleagues (1991, 1993), who observed an analogous actin purse-string that appears to drive the natural morphogenetic movement of dorsal closure in *Drosophila* embryos whereby the lateral epidermis sweeps in over the amnioserosa of the embryo. In *zipper* mutant embryos that lack a functional copy of the zygotic myosin II gene, dorsal closure fails (Young et al., 1993).

In the current paper we analyze the time course of assembly of filamentous actin at the embryonic wound edge, of the adherens junction proteins that serve as anchorage for intracellular segments of the actin cable, and of the myosin molecules that act as the motors for actin contraction. Having observed that this contractile machinery assembles very soon after wounding, within the first few minutes, we go on to investigate how such rapid reorganization of the cytoskeleton might be regulated. Equally rapid reorganizations of the actin cytoskeleton occurring in Swiss 3T3 fibroblasts after exposure to various growth and serum factors recently have been shown to be mediated by the Rho family of small GTPases including Rho, Rac, and Cdc42 (for review see Hall, 1994). By microinjection of a dominant-negative mutant Rac protein, Ridley et al. (1992) showed that Rac is specifically required for rapid polymerization of actin at the plasma membrane to form lamellipodia in response to growth factor signals. They also showed that activation of the related small GTPase, Rho, is required for assembly of actin stress fibers and associated focal adhesion complexes in fibroblasts exposed to serum after a period of serum starvation, since cells previously injected with the bacterial exoenzyme C3 transferase, which ADP-ribosylates and thus inactivates endogenous Rho, completely fail to respond to serum in this way (Ridley and Hall, 1992). A third member of the Rho family, Cdc42, recently has been shown to mediate rapid extension of filopodia and the accompanying localized actin polymerization in Swiss 3T3 fibroblasts (Nobes and Hall, 1995).

These in vitro observations suggest that the Rho proteins are likely to be key molecular switches governing various steps in reorganization of the cytoskeleton during concerted tissue movements such as those of embryonic morphogenesis or wound healing. Indeed, a number of recent papers suggest that these GTPases may be important regulators of morphogenetic movements in *Drosophila*. If *Drosophila rho1* is overexpressed in the eye, then dramatic abnormalities in the ommatidial architecture of the retina result, due to a failure of critical cell shape changes as the morphogenetic furrow sweeps across the developing eye (Hariharan et al., 1995). Similarly, interfering with normal Rac function by targeted expression of constitutively active or dominant inhibitory *Drosophila rac1* causes various disruptions of morphogenesis including impaired germ band retraction and dorsal closure (Harden et al., 1995), and also disrupts later events such as axon elongation and myoblast fusion (Luo et al., 1994).

Might one of the Rho family of proteins also be responsible for mediating the assembly of an actin purse-string at the edge of an embryonic wound? To test this possibility, we have taken advantage of the fact that embryonic wound edge cells—precisely those cells that would normally go on to assemble an actin cable—become briefly leaky at the the time of wounding and so become "scrape loaded" with reagents supplied in the extracellular medium. We have used this approach to load the wound edge cells either with dominant-negative mutant Rac protein, N17rac, or C3 transferase, the Rho-blocking agent. The Rho-inhibiting treatment, but not the Rac-inhibiting treatment, blocks both actin cable assembly and the subsequent wound closure movements, suggesting that Rho may be the molecular switch mediating the wound-induced signal for assembly of an actin cable, whose contraction drives wound closure.

Materials and Methods

Wounding

Fertilized chicken eggs (White Leghorn from Needle Farm, Herts, UK) were incubated at 38 ± 1°C and windowed at approximately stage 18 in preparation for wounding at stage 23 (Hamburger and Hamilton, 1951). A previous study of chick embryo wound healing involved excisional wounds where small patches of skin were dissected away (Martin and Lewis, 1992). These lesions take up to 10 min to create, which makes it difficult to look at the very earliest stages of healing (within minutes after wounding). To circumvent this problem, in the present study we have made simple longitudinal cuts to the dorsum of the chick wing bud using an electrolytically sharpened tungsten needle. For our time course studies, three uniform "slash" lesions, ~500 μm long, were made in the limb bud at different time points, each lesion parallel to the proximodistal axis of the bud, with the earliest lesion placed anteriorly, the second lesion in the middle, and the last lesion posteriorly (see Figs. 1 *A* and 2 *A*). Between each wounding, embryos were returned to the incubator to allow healing to continue at 38°C. Immediately after the third and final wounding, embryos were fixed by squirting fixative onto the embryo in ovo, allowing us to compare, on each limb, "0-h" lesions with lesions that had been left to heal for two additional periods of time. In this way, we examined wounds that had been healing for 0, 2, 5, 10, 15, and 30 min, and 1, 2, 3, and 6 h. For our Rho- and Rac-blocking experiments (see later), two or three smaller incisional wounds were made within seconds of one another to each limb bud.

Scanning Electron Microscopy and Resin Histology

Wounded embryos were fixed initially in half-strength Karnovsky's fixative (Karnovsky, 1965), and then post fixed in 1% osmium tetroxide in 0.1 M cacodylate buffer, dehydrated in a graded series of alcohols, critical-point dried, and sputter coated with gold in preparation for scanning electron microscopy (SEM).[1] Our microscope was a Philips SEM 515 (Philips Electronic Instruments, Inc., Mahwah, NJ). A small number of embryos were fixed also in half-strength Karnovsky fixative, postfixed in osmium tetroxide, dehydrated, and embedded in Araldite for routine resin histology. Sections were cut at between 1 and 5 μm and stained with Toluidine blue.

Actin Staining and Confocal Laser Scanning Microscopy

Whole embryos were fixed in 4% paraformaldehyde in PBS, rinsed in PBS, soaked overnight in a mix of FITC-phalloidin (100 ng/ml; Sigma Chemical Co., St. Louis, MO) (Wulf et al., 1979) and the nuclear dye

1. *Abbreviation used in this paper*: SEM, scanning electron microscopy.

7-aminoactinomycin D (10 μg/ml; Molecular Probes, Eugene, OR) in PBS, rinsed thoroughly, and mounted in Citifluor (Chem Labs, Canterbury, UK) under a coverslip to flatten the limb surface and to bring the whole wound area into the same plane of focus. These wounds were then viewed with either an MRC 600 (Bio Rad Laboratories, Hercules, CA) or a TCS-4D (Leica Inc., Deerfield, IL) confocal laser scanning microscope to reveal the distribution of filamentous actin and nuclei in the cells of the wound margin.

To examine the time course of actin cable formation quantitatively, we made measurements with the confocal scanning microscope. Focusing on the plane in which the cable appeared clearest, we used the standard image analysis software provided with the microscope to measure the intensity of the fluorescence along a rectangular strip drawn perpendicular to the wound edge, and to plot the mean intensity in this strip as a function of distance from the wound edge, as shown in Fig. 4. For all but the time 0 wounds, the graph showed a clearly defined peak of fluorescence corresponding to the actin at the wound edge. The amount of actin in the cable was estimated by integrating the signal over a 3-μm interval centered on this peak. (This is very roughly the width of a typical peak at half height.) We compared this value with the corresponding value in the tissue to the rear of the wound front, averaged over a 20-μm interval between 5 and 25-μm from the front. We refer to the ratio of the two values as the actin concentration ratio: presence of a cable is reflected in ratios >1.

Immunocytochemistry

To further characterize the contractile machinery, we investigated the localization of cadherins and myosin II (essential for actin cable anchorage and contraction, respectively) by whole-mount immunohistochemistry. Wounded embryos were fixed in 4% paraformaldehyde, rinsed in PBS (with 0.3% Triton), and incubated, with agitation, for 2 h at room temperature with the appropriate primary antibody. For myosin visualization, we used a murine anti-myosin antibody (Sigma Chemical Co.) at 1:200 dilution, and to visualize cadherins, we used a rabbit anti–pan-cadherin antibody (Sigma Chemical Co.) also at 1:200. Primary antibodies were revealed using FITC-tagged goat anti–mouse and goat anti–rabbit antibodies, respectively, both at 1:200 dilutions (Pierce Chemical Co., Rockford, IL). Embryos were then thoroughly rinsed in PBS and counterstained with the nuclear dye 7-aminoactinomycin D (10 μg/ml; Molecular Probes). Subsequent mounting and confocal laser scanning microscopy of these specimens was precisely as described above for actin-stained specimens. Those embryos in which primary or secondary antibodies were omitted showed no localized background staining.

Rho- and Rac-blocking Experiments

To test the role of the small GTPases Rho and Rac in embryonic re-epithelialization we scrape loaded wound edge cells at the time of wounding either with the bacterial exo-enzyme C3 transferase (gift from Catherine Nobes, University College London, UK) that ADP-ribosylates and thus inactivates endogenous Rho (Paterson et al., 1990), or with myc-tagged N17 rac, a mutated form of Rac that blocks normal Rac function (Ridley et al., 1992; gift from David "Dusty" Drechsel, University College London, UK). To first demonstrate that epithelial cells at the wound margin are made transiently permeable by wounding, we pipetted 10 μl of 20 mg/ml lysinated (fixable) 10- and 40-kD TRITC-dextrans (Molecular Probes) onto the surface of the limb bud before wounding. The brightest fluorescent cells loaded in this way appeared approximately equivalent in brightness to 3T3 fibroblasts microinjected with 2 mg/ml of dextran. This would suggest that scrape loading reagents of <40 kD into wound margin cells in ovo is approximately one-tenth as efficient as microinjection, and since microinjection increases a cell's volume by between 10 and 25% (Nobes, C., personal communication), this would suggest that scrape loading results in a final intracellular concentration of ~1–2% of the original applied concentration of the reagent. Such dextran-loaded specimens were fixed in 4% paraformaldehyde in PBS within seconds of wounding or at 30 min or 3 h after wounding. They were subsequently counterstained with FITC-phalloidin to reveal actin and viewed under the confocal laser scanning microscope as described above. If the dextrans are applied to the limb surface a few minutes after wounding, rather than before, almost no cells become loaded (data not shown), implying that cells are only transiently leaky at the time of wounding. For the Rho-blocking experiment, wounds were made in the presence of C3 (10 μl of 100 μg/ml) and TRITC-dextran (same concentration as above), and they were examined either by staining for actin with FITC-phalloidin and viewing by confocal laser scanning microscopy at 30 min and 3 h after wounding, or by SEM at 3 and 6 h. For the Rac-blocking experiment, wounds were made in the presence of myc-tagged N17rac (10 μl of 1 mg/ml). Embryos were fixed and either costained with TRITC-phalloidin and FITC-tagged goat anti–mouse antibody (1:300) + mouse anti–myc antibody (1:300) (two additional gifts from "Dusty" Drechsel) to reveal the cells that had taken up N17rac at 30 min and 3 h after wounding, or viewed by SEM after 3 and 6 h to determine the extent of healing.

Results

To examine the normal time course of wound closure, we made three cuts to the dorsum of each wing bud, at three different times, with the last of them immediately before fixation. In this way, we could compare, in a single specimen, the extent of healing and the changes in actin, cadherin, and myosin distribution in epidermal wound front cells at different times after wounding.

Wounds Are Generally Healed by 6 h with the Epidermis Apparently Zipping Closed

The mean length of a sample of 17 wounds measured from scanning electron micrographs at time 0 was 490 ± 30 μm (mean ± SD). Already, within seconds after the operation, these wounds had gaped to a mean width of 70 ± 30 μm (mean ± SD). The needle had not always cut cleanly through the tissue, and the resulting irregularities meant that the extent of gaping was variable along the length of a single wound. The initial depth of the wounds was assessed from transverse sections and found to be ~150 μm. This is deeper than the level at which the cutaneous vascular plexus forms (~100 μm beneath the epidermis (Caplan and Koutroupas, 1973; Martin and Lewis, 1989), and, as a result, all of our lesions resulted in some bleeding. Since we remove no tissue when we make our cuts, gaping reflects elastic recoil of the mesenchyme and epidermis on either side of the cut.

The initial trench in the mesenchyme became filled in and narrowed, presumably through the cohesiveness and contractile behavior of the mesenchyme cells. By 1 h the trench was filled in and the opposite epidermal edges of the wound epidermis faced one another across a smooth, narrow strip of denuded mesenchyme (Figs. 1 *E* and 2 *C*). Often, at a few sites, the epidermal edges came into direct contact and adhered to one another. From these points, and from the two ends of the wound, the epidermis appeared to zip closed, so that the wound closed by shortening from its ends toward the center. Behind the zipper front, one could see by SEM a seam line, where the peridermal cells were oriented with their long axes parallel to the original wound edges (Fig. 1 *C*). Further back from the zipper front, the seam began to fade out and blend with unwounded periderm so that the line of healing was no longer superficially visible.

By 6 h almost all of the wounds we looked at had closed completely; those remaining open usually appeared blocked by collections of cellular debris. In closed and almost closed wounds, the wound site was often still visible as a raised epidermal ridge, with local disorganization of the periderm (Fig. 1 *H*). Beneath this closed seam there remained significant mesenchymal disorganization, and there was often a pocket of cellular debris within the wound cleft that had not yet been cleared away (Fig. 2, *C* and *D*).

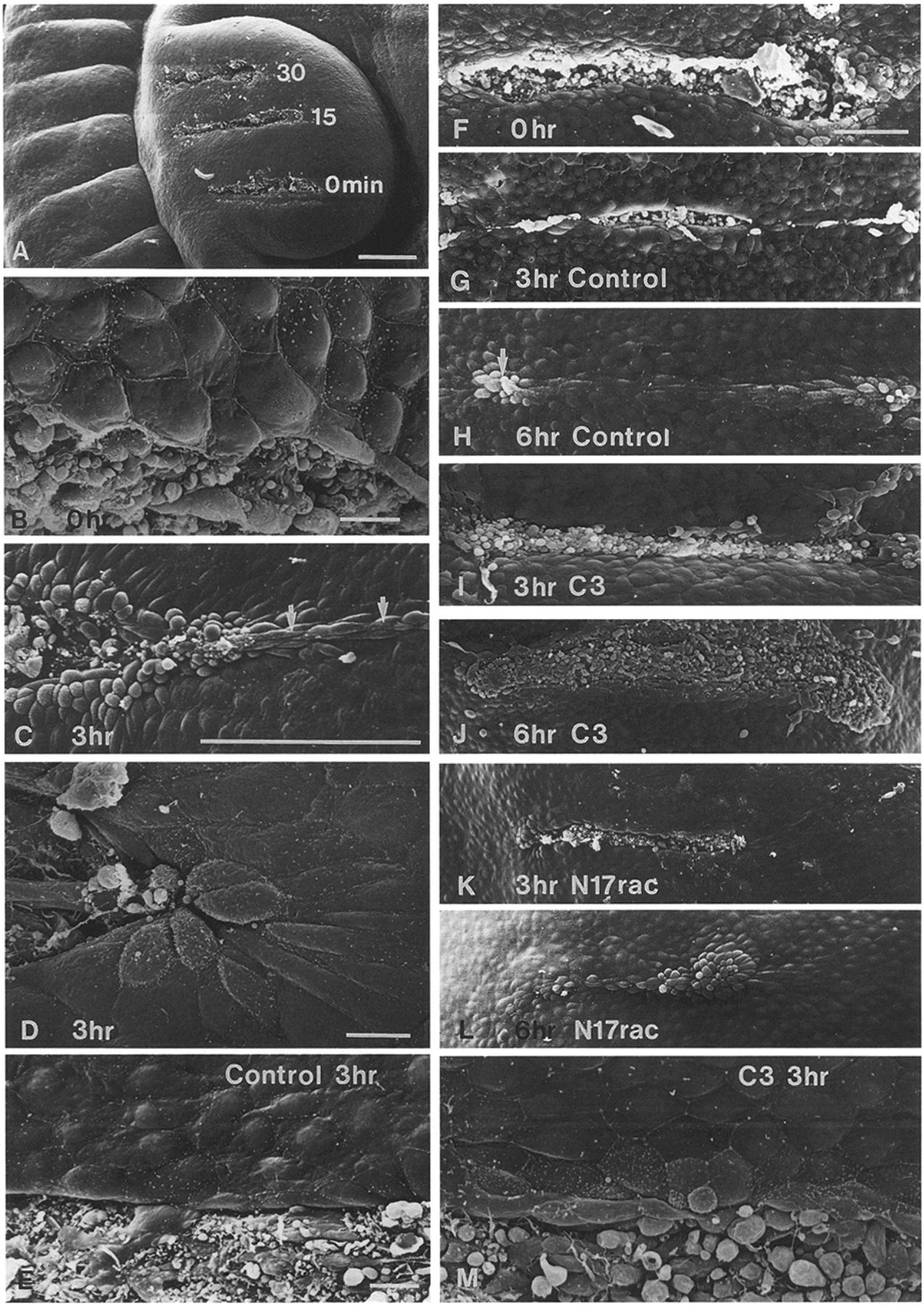
30
15
0min
A
B 0hr
C 3hr
D 3hr
Control 3hr
E
F 0hr
G 3hr Control
H 6hr Control
I 3hr C3
J 6hr C3
K 3hr N17rac
L 6hr N17rac
C3 3hr
M

The detailed appearance of the epidermal wound margin during the healing of these incisional wounds was similar to that seen previously for excisional wounds (Martin and Lewis, 1992). At time 0 the cut edge appeared ragged, with many of the cells damaged and some cleanly cut in half (Figs. 1 *B* and 2 *B*), but within 10 min the wound margin had smoothed out considerably, with swollen peridermal cells clothing the wound edge. By 1 h the wound margins had become smoother still (Fig. 1 *E*). At the two ends of the wound, the peridermal cells were often arranged radially around the endpoints, with their long axes perpendicular to the wound margin (Fig. 1 *D*); this state of affairs persisted until the wound was closed.

At no stage during the healing process did the peridermal cells show any sign of lamellipodia or filopodia extending from their free edges. Neither were any such processes visible, poking out beneath the peridermal cells, from the basal epidermal layer of cells. These observations using SEM were confirmed in transverse resin section that showed the epidermal fronts to be blunt faced (Fig. 2 *C*). As we have previously reported for excisional lesions (Martin and Lewis, 1992; McCluskey and Martin, 1995), lamellipodial crawling does not appear to be the mechanism of healing of the embryonic epidermis.

An Actin Cable Forms at the Wound Edge within Minutes after Wounding

To examine the distribution of filamentous actin in and around the wound, we stained our specimens with fluorescently tagged phalloidin and used confocal scanning microscopy to view thin optical sections in the plane of the wound (i.e., parallel to the limb-bud surface). At all stages, filamentous actin could be seen in the cortical cytoplasm of the cells, outlining, for example, the peridermal cells that form a pavement on the outer surface of the epithelium (Fig. 3 *A*).

In a fresh (0-h) wound, fixed <30 s after cutting, there was no visible specialization of the actin distribution at the wound margin in any cell layer—peridermal, basal epidermal (Fig. 3 *E*), or mesenchymal. In wounds fixed only 2 min later, a concentration of actin had begun to be visible along the wound edges in the basal epidermal cells (Fig. 3 *F*). This band of actin was at first hazy and discontinuous at many sites. By 5 min it had become more sharply delineated as a thin cable or strand, appearing continuous from basal cell to basal cell around most of the wound margin (Fig. 3 *G*). By 30 min it had attained its full thickness, which it retained until the final stages of wound closure (Fig. 3, *B* and *I*).

For at least four samples of wound margin from each of a series of time points from 0 to 3 h after wounding, we measured the quantity of actin in the cable, as indicated by the actin concentration ratio at the wound edge (see Materials and Methods). The mean values of the actin concentration ratio are plotted in Fig. 4 as a function of time. The maximum ratio is ~4.0; this value is attained within 30 min after wounding and does not change significantly thereafter. A value of 3.0, i.e., a trebling of the normal actin concentration, is seen already 5 min after wounding, although the cable seen at this stage still has a somewhat immature appearance, and the edges of the wound have not yet become smooth and regular.

The Actin Cable Disassembles at Sites where Opposite Wound Edges Have Made Contact

Upon examining the zipped-up portions of 3- and 6-h wounds, we found that the cable had largely disassembled in regions where the opposite epidermal edges had come together, leaving just remnants of the actin cable extending three or four cells back in the freshly closed seam. The remnants of actin cable in the wake of the zipper were variable in extent and organization. Sometimes the actin, while still plentiful, appeared disorganized; sometimes it was still oriented along the axis of the wound (Fig. 3 *H*). In wounds that had recently closed, we found that the actin cable had fully disassembled, but that a concentration of disorganized actin remained as a marker of where the wound had been (Fig. 3 *J*). Even this remnant of the healing machinery had disappeared by 12 h after wounding.

Cadherins Become Rapidly Clustered at Adherens Junctions between Neighboring Wound-Margin Cells

Since the actin cable must in fact consist of many individual intracellular segments of cable linked to one another by cell–cell adherens junctions, we looked by confocal microscopy at the pattern of staining with an antibody raised against cadherins, the transmembrane adhesion component of all adherens junctions (Tsukita et al., 1992). Association of cadherins into large cell junctional clusters was restricted to the leading edge of basal front row cells (Fig. 3 *C*), coincident in time and location with the actin cable assembly. These clusters were resolvable from ~2–5 min after wounding along the full extent of the wound edge

Figure 1. Scanning electron micrographs to show wound healing in control and treated wounds. (*A*) Low magnification SEM view of wing bud with three healing lesions. The embryo was fixed when the most posterior (bottom) lesion had been healing for 0 min, the middle lesion for 15 min, and the most anterior (top) lesion for 30 min. (*B*) A high magnification view showing the rough wound edge at 0 h. (*C*) Detail from a 3-h lesion revealing a long stretch of zipped-up wound. The wake of the zipper is revealed by a raised seam of oriented peridermal cells (*arrows*). (*D*) Detail from a closing wound revealing the radial orientation of peridermal cells at one end of a region of purse-string wound closure. (*E*) The smooth epithelial margin in a region of 3-h wound; the peridermal cells appear taut and stretched out around the closing wound margin. (*F*) A typical 0-h wound. (*G*) A control, untreated wound showing significant closure after 3 h. (*H*) A healed 6-h lesion showing the remaining vestiges of the closure process, the closed seam and some extruded cell debris (*arrow*). (*I*) By comparison, a C3-treated wound has not reepithelialized after 3 h. (*J*) Even at 6 h C3-treated wounds have not closed, and this example appears to have gaped open even further. (*K*) After 3 h N17rac-treated wounds are closed to the same extent as control wounds. (*L*) After 6 h N17rac-treated wounds are fully closed. (*M*) Detail from a C3-treated 3-h wound, showing a region where the peridermal margin appears slack and not under the same tension as that seen at an untreated wound margin (compare with *E*). Bars: (*A*) 200 μm; (*B*, *D*, *E*, and *M* [same magnification]) 10 μm; (*C*) 100 μm; (*F–L* [same magnification]) 50 μm.

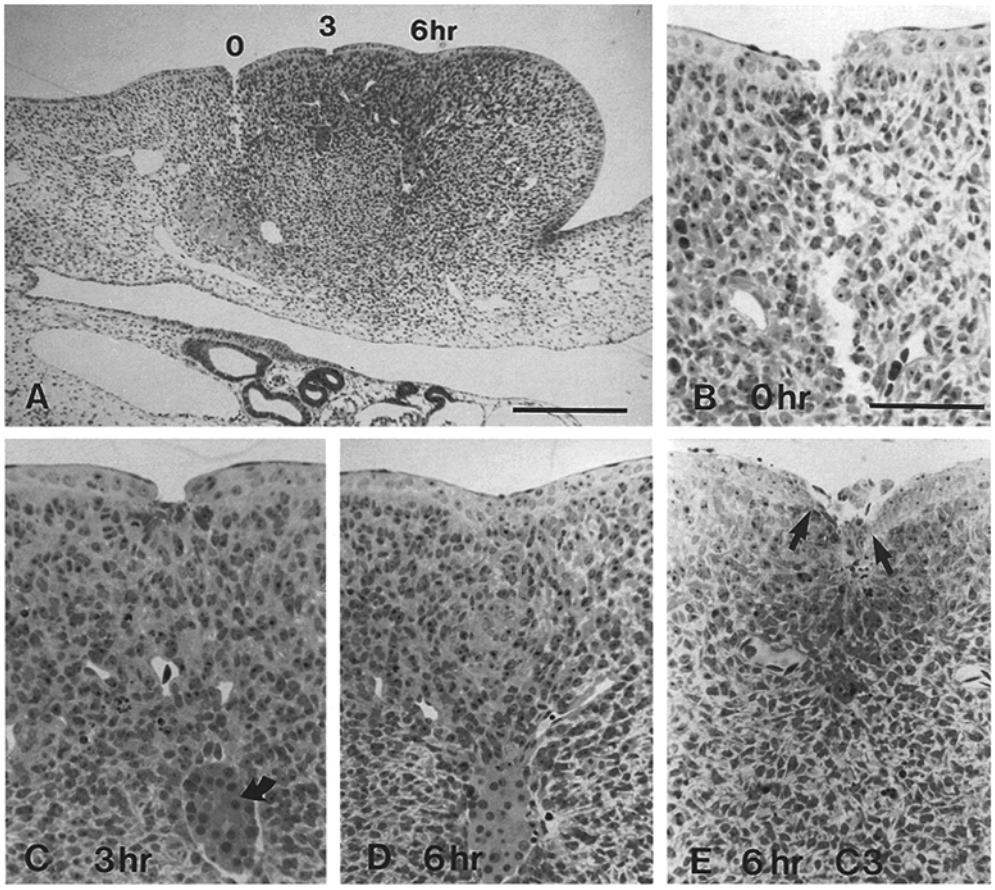

Figure 2. Resin histology of control and C3-treated wounds. (*A*) Transverse resin section through a wounded wing bud similar to that shown in Fig. 1 *A*. The embryo was fixed when the most posterior (*left*) lesion had been healing for 0 min, the middle lesion for 3 h, and the most anterior (*right*) lesion for 6 h. (*B–D*) are all details from *A*. (*B*) Higher magnification view of 0-h lesion, revealing irregular epidermal and mesenchymal wound edges. (*C*) Detail of a 3-h wound, revealing rounded, blunt-faced, epidermal wound fronts; the mesenchymal gap has now been filled in, but note a pocket of RBCs where the base of the wound had been (*arrow*). (*D*) Detail of a 6-h wound. The epidermis has fully closed over the wound. (*E*) High magnification view of a C3-treated wound at 6 h where the wound edges (*arrows*) are still apart from one another. Bars: (*A*) 200 μm; (*B–E* [same magnification]) 50 μm.

and persisted throughout the duration of wound closure. At later time points during healing, in regions of wound that had zipped up, we saw cadherin clusters extending only about one- or two-cell diameters beyond the open wound, suggesting that the cadherins disaggregate as the actin cable disassembles (data not shown).

Myosin Localizes to the Site of the Actin Cable at the Wound Margin ~10 min after Wounding

The actin cable clearly requires myosin motors if it is to be contractile, and thus we have investigated the presence of nonmuscle myosin II at the wound border, again using confocal microscopy. We found antibody staining for myosin II in the leading edge of basal wound epidermal cells, with a distribution reminiscent of the actin purse-string itself (Fig. 3 *D*). As with the actin cable, no myosin cable was seen in the peridermal wound edge cells at any stage during wound closure, or in the basal epidermal layer at 0 h. In the basal cells, myosin took somewhat longer than actin or cadherins to become localized to the wound edge; the earliest we saw a clear myosin cable was 7 min after wounding.

Loading Wound Edge Cells with the Rho-blocker C3 Transferase Prevents Assembly of an Actin Cable and Subsequent Reepithelialization

To test whether the small GTP-binding proteins Rho or Rac might be mediating assembly of the actin cable in embryonic wound epithelial cells, we loaded cells at the time of wounding with fluorescent dextrans (as a marker) together with either C3 transferase that blocks endogenous Rho function, or with myc-tagged dominant-negative N17rac protein. Control experiments, in which only fluo-

Figure 3. Confocal laser scanning microscopy of healing epithelial wounds on the dorsum of the chick wing. (*A*) Superficial peridermal layer of the epithelial wound edge 30 minutes after wounding stained with FITC-tagged phalloidin (*green*) and the nuclear dye 7AAD. (*B*) Basal epithelial layer of the same wound edge. An actin cable is clear at the leading edge (*arrows*). (*C*) Basal epithelial wound edge immunolabeled with pan-cadherin antibody (*green*) and 7AAD. Note clusters of cadherins (*arrows*) localizing to adherens junctions along the leading epithelial edge. (*D*) Confocal image of the basal epithelial layer of a 30-min wound immunolabeled to reveal myosin II (*green*) and counterstained with 7AAD. Myosin is localized to the leading edge (*arrows*) just as actin is. (*E*) Confocal image of the basal wound epithelium as in *B* but at Ohr. There is no cable present. (*F*) At 2 min after wounding, a thin cable is becoming visible. (*G*) By 5 min a distinct cable is present. *H* shows a region of a closing 3-h wound stained with FITC-phalloidin and 7AAD. An oriented remnant of the cable lies along the seam where zipping-up has occurred (*arrows*). (*I*) A 6-h wound that has almost closed reveals an actin cable of only 2–3-cell diameters just before full wound closure. (*J*) Just after the wound has finally closed, there remains a trail of disorganized actin along the wound seam. *m*, exposed mesenchyme. Bars: (*A–D* [same magnification]; *E–G* [same magnification]; *I* and *J* [same magnification]; *H*) 20 μm.

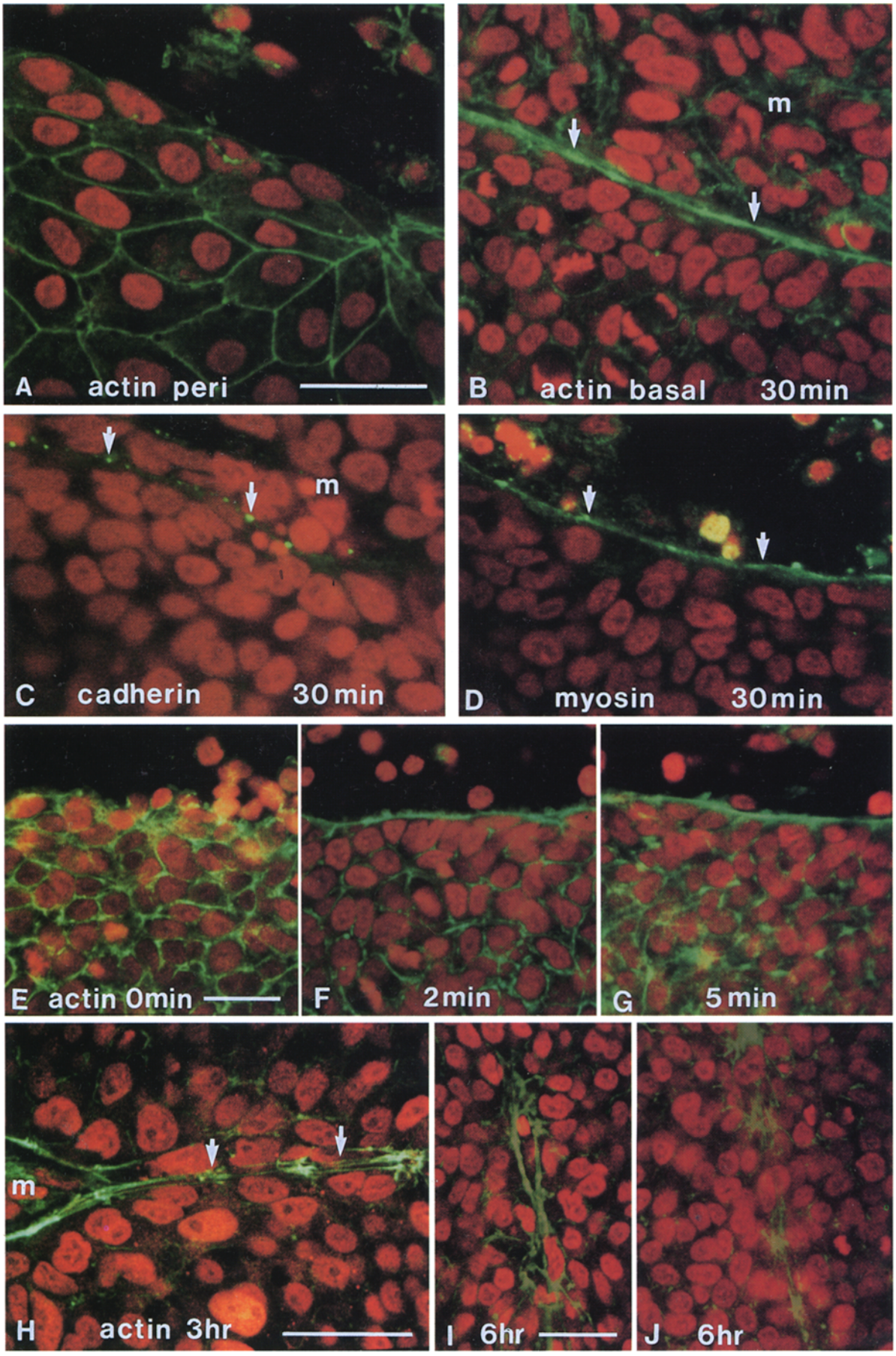
A actin peri
B actin basal 30min
m
C cadherin 30min
m
D myosin 30min
E actin 0min
F 2min
G 5min
H actin 3hr
m
I 6hr
J 6hr

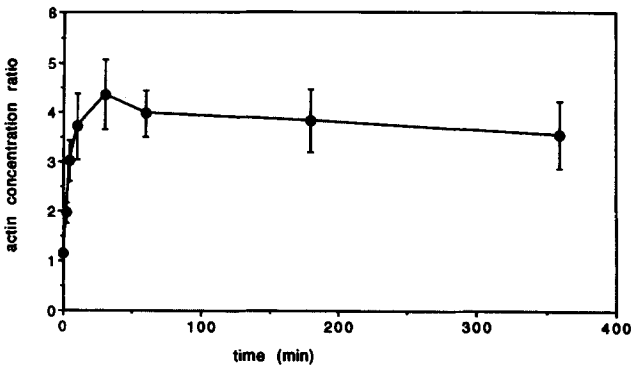

Figure 4. Actin cable formation as a function of time after wounding. The amount of actin in the cable is represented by the actin concentration ratio, i.e., by the ratio of the density of actin in the cable to the density of actin elsewhere in the epithelium (measured as described in Materials and Methods). The error bars show the SEM of measurements from at least four samples of wound edge for each time point.

rescent dextran was dripped onto the dorsum of the wing bud just before wounding and embryos harvested a few min later, showed that it was possible to load between ~50–70% of basal wound edge cells in this way (Fig. 5 *A*). Moreover, in similarly treated control embryos allowed to heal their wounds for 3 h, it was clear that dextran loading on its own had no detrimental effect on either actin cable assembly or subsequent wound closure (Fig. 5 *B*). After 3 h of incubation in regions where the wound epithelium had healed, labeled cells, which had initially been at the wound edge, were now seen to lie in a trail along the closed epithelial seam, confirming our impression from the SEM data reported above that these wounds generally close by drawing wound edges together in a zipper-like fashion (Fig. 5 *B*).

In experiments where we coloaded C3 transferase (applied at 100 μg/ml) with fluorescent dextrans and left wounds to heal for 3 and 6 h, it was clear that all of the labeled cells had failed to assemble an actin cable, but that the majority of unlabeled neighboring wound edge cells had segments of actin cable present at their leading edges (Fig. 5, *C* and *E*). When applied to the limb surface at 10 μg/ml, most C3-loaded cells assembled a feeble-looking cable, and at lower concentrations still, cable assembly was as in untreated wounds (data not shown); all subsequent experiments were performed at 100 μg/ml. Our blocking experiments indicate that Rho activation is required to mediate wound-induced assembly of an actin purse-string. C3-treated specimens showed very little sign of having closed their wounds by 3 h (Fig. 1 *I*) and were still not reepithelialized at 6 h (Fig. 1 *J*), by which time control wounds have fully closed (Fig. 1 *H*). Measurement from scanning electron micrographs of 18 such treated wounds revealed the length of incision remaining open at 3 h to be 87 ± 5% (mean ± SEM) of the mean original wound length, compared with 42 ± 7% (mean ± SEM) remaining open in control untreated wounds. After 6 h, by which time all control wounds have closed, the 15 C3-treated wounds were still 91 ± 5% (mean ± SEM) of the initial mean length. Scanning electron microscopy views of the leading edge of C3-treated wounds at 1 and 3 h generally revealed little effect on periderm cell morphology, except that in some regions of C3-treated wounds the peridermal margin was clearly slack (Fig. 1 *M*) by comparison with the taut leading edge of a control wound (Fig. 1 *E*). Histologically, C3-treated epidermal wound fronts appeared somewhat more flattened (Fig. 2 *E*) by comparison with control wound edges (Fig. 2 *C*).

Similar experiments loading myc-tagged N17rac into wound edge cells failed to disrupt actin cable assembly (Fig. 5, *F* and *G*), suggesting that Rac is not required for this. Embryos treated with 1 mg/ml N17rac healed their wounds with normal time course, not significantly different from control wounds (Fig. 1, *K* and *L*). At 3 h, N17rac treated wounds had closed to 30 ± 14% (mean ± SEM; n = 4) of original wound length, and after 6 h (n = 4) all wounds were closed. Although we have no direct proof that the uptake of N17rac was sufficient to block Rac function in our system, we have titrated the same preparation of myc-tagged N17rac by microinjection into Swiss 3T3 fibroblasts and found that it is still functional at blocking PDGF-induced ruffling when microinjected at concentrations as low as 0.1 mg/ml. Moreover, in 3T3s the myc-tag could only be detected when microinjected at higher concentrations than the minimal functional concentration, suggesting that in our in vivo experiments, the bright myc-staining reflects uptake of sufficient protein to block endogenous Rac signaling.

Discussion

In this study we investigate epithelial healing of incisional wounds made in vivo to the surface of the chick embryo wing bud. These wounds appear to heal by a combination of two processes: the wound margin shortens by a contractile action of the basal epithelial cells at the wound margin; at the same time, the cut edges of epithelium on opposite sides of the incision become joined together again, much as two pieces of cloth are drawn together by a zipper.

Healing of the incisional wound, like that of an excisional wound, is associated with the formation of an actin cable in the basal epithelial cells at the wound margin. We have shown that this cable assembles within minutes of wounding and that it rapidly recruits myosin, making it potentially contractile. Formation of the cable is blocked by a reagent that specifically inactivates Rho, a key regulator of actin stress fiber assembly. The result of this treatment is that the wound fails to heal, as predicted if the actin cable is a necessary part of the machinery for wound closure. The failure of epithelial healing is almost total, implying

Figure 5. Confocal laser scanning microscopy of wounds loaded with TRITC-dextran and either C3 transferase or N17rac to block Rho or Rac signaling. (*A*) TRITC-dextran–loaded basal epithelial cells (*red*) at the margin of 0-h wound (*arrows*). Actin is stained with FITC-tagged phalloidin (*green*). (*B*) Similar wound to *A*, but allowed to heal for 3 h. All cells at the wound margin, whether dextran labeled (*arrow*) or not, have assembled actin cable (*green*). Some of the cells initially labeled at the wound margin now lie along the healed seam (*white spots*). (*C*) Wound edge cells coloaded with TRITC-dextran (*red*) and C3 transferase at the time of wounding and al-

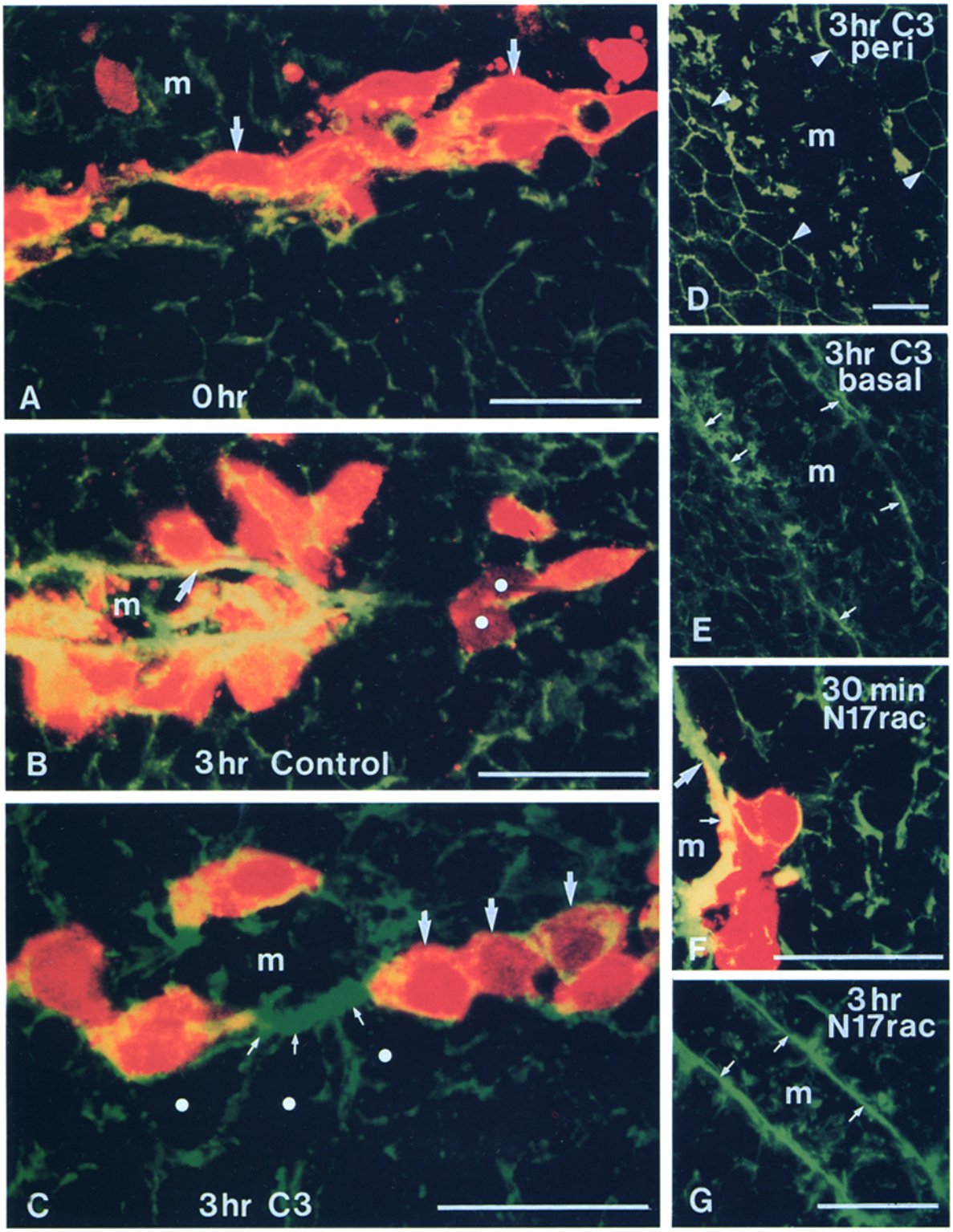

lowed to heal for 3 h. Note that loaded wound edge cells (*red*, e.g., those indicated by large arrows) do not contain actin cable, while neighboring cells that were not loaded (*white spots*) have assembled intracellular segments of cable (*small arrows*). (*D* and *E*) Lower magnification views of another 3-h C3-treated wound (stained with FITC-phalloidin) imaged at the level of the periderm and the basal epidermal layers, respectively; *D* shows the extent that the two peridermal wound edges (*arrowheads*) are still apart; *E* reveals that a majority of basal cells at the leading edge fail to assemble an actin cable (compare with Fig. 3, *B* and *I*); however, occasional cells (presumably those not loaded with C3) have assembled segments of actin cable (*arrows*). (*F*) Wound edge cells loaded with FITC myc-tagged N17rac (confocal channel luted to red) at the time of wounding and allowed to heal for 30 min. Actin cable has assembled in both labeled (*small arrow*) and unlabeled (*large arrow*) cells at the wound edge. (*G*) Two opposing wound margins (*arrows*) of a 3-h, almost closed, N17rac-treated wound stained only with FITC-phalloidin, showing actin cable assembly in all basal epidermal cells at the leading edge. *m*, exposed mesenchyme. Bars: (*A*, *B*, *C*, *D*, and *E* [same magnification]; *F* and *G*) 20 μm.

that both components of the process have been prevented—both the wound margin contraction and the zipping up. This suggests that in normal healing the actin cable provides the contractile force not only to constrict the wound margin by a purse-string action, but to pull on the zipper that draws the wound edges together.

Formation of the Actin Cable at the Wound Margin

In our previous study of excisional wounds in the chick embryo (Martin and Lewis, 1992), we were unable to follow the early time course of actin cable assembly because these wounds took some time to make. The present study of incisional wounds has allowed us to observe, in vivo, the early steps of the process. An actin cable assembles within 2 min after making a cut and reaches full size within 30 min. The actin cable must actually consist of intracellular actin segments stretching the length of every cell at the epithelial wound margin, each intracellular segment being linked to its two neighbors via cell–cell junctions. Indeed, our cadherin immunocytochemistry suggests that large adherens junctions assemble around the wound margin with similarly rapid time course to the actin cable and presumably serve as the anchor points for this cable. We first see localization of myosin to the wound edge between 7 and 10 min after wounding, a few minutes after the actin cable has formed, suggesting that myosin localization is dependent on actin cable assembly, as one might expect. The time course that we observe for both actin and myosin is almost identical to that reported by Bement et al. (1993) in their in vitro wounds. In both systems, the initial formation of the cable seems too rapid to depend on new synthesis of actin or actin mRNA. The actin cable must instead form at first by reorganization of existing filamentous actin or polymerization of existing actin monomers.

The small GTP-binding protein Rho has been shown to act in cultured fibroblasts as a regulator of actin stress fiber assembly on a similarly rapid time scale (Ridley and Hall, 1992), and our C3 transferase scrape-loading experiments suggest it plays a similar role in regulating assembly of an actin purse-string—essentially a collection of oriented actin stress fibers—in the cells of the embryonic epithelial wound margin. When we load wound edge cells with dominant-negative N17rac protein, to disrupt Rac function, we see neither an effect on actin cable assembly nor any disruption of epithelial healing. Our observations are in accordance with those of Ridley et al. (1995) who report that peripheral actin bundles at the margin of cultured islands of MDCK epithelial cells are not disrupted by N17rac, but disassemble after injection with C3. However, these observations contrast somewhat with two experiments in *Drosophila.* Eaten and colleagues (1995) genetically disrupted *rac* during a period of active morphogenesis in the wing imaginal disk and found that this interfered with the anchorage of actin into newly forming adherens junctions in some regions of the wing epithelium. Dominant negative *rac* under the regulation of a heat shock promoter has also been shown to interfere with dorsal closure in the *Drosophila* embryo, an effect that correlates with decreased actin in the leading edge of dorsally spreading epithelia (Harden et al., 1995).

While our studies suggest that Rho is required for assembly of an actin purse-string and subsequent reepithelialization of an embryonic wound, we would predict that reepithelialization of adult skin wounds, which involves actin-driven lamellipodial crawling of basal keratinocytes rather than purse-string contraction, would instead be dependent on the small GTPases Cdc42 and Rac, which mediate extension of filopodia and lamellipodia, respectively, in cultured cells (Ridley et al., 1992; Nobes and Hall, 1995).

What Might Activate Rho in Wound Edge Epithelial Cells?

In cultured fibroblasts Rho can be activated by serum stimulation or by mechanical signals such as vibration (Ridley and Hall, 1992; Nobes, C., personal communication). When we wound the embryonic skin, it is clear that basal epithelial cells at the leading edge will be immediately bathed by various factors in the amniotic fluid that they are not directly exposed to as part of an intact epithelium covered with a layer of peridermal cells; these factors might provide an actin reorganization signal. However, we believe that the more likely primary stimulus for actin reorganization in wound edge cells is a change in the pattern of stresses in the epidermis, rather than a ligand/receptor-mediated signal. The unwounded embryonic epidermis is evidently under tension since it gapes when it is cut. By making a cut, we relieve the cells on either side of the cut from the component of tension acting at right angles to the wound margin, while retaining the component of tension parallel to the wound margin. Kolega (1986) has previously shown that pulling on cultured epidermal cells provokes alignment of actin filaments along the principal axis of stress and suppresses lamellipodial activity at right angles to that direction. The cells at the cut edge of our wounded embryonic epidermis appear to behave according to the same rules. It will be fascinating to determine more directly whether stretch is indeed the stimulus that triggers Rho activation and subsequent assembly of an actin cable, or whether it merely orientates actin filaments that have polymerized in response to other signals.

Zipping-up and the Formation of New Contacts between Epithelial Cells during Healing

As a wound closes, the length of epidermal free edge around the perimeter of the wound decreases. If there were no changes in cell–cell contacts, so that the number of cells in the wound margin remained constant, this would have to correspond to a narrowing of the segment of perimeter formed by each cell, converting the cell to an inward-pointing wedge shape. But, in fact, as we reported earlier in our study of excisional wounds (Martin and Lewis, 1992) and show again in this study, although occasional wedge-shaped cells are seen along the straight edges of the wound margin, in general the average shape of wound edge cells does not appear to change significantly as the wound closes, except perhaps at sites where the wound is very sharply curved (as at the two ends of our incisional wounds). It follows that wound closure must involve changes in cell–cell contacts and not just changes in cell shape. The present study reinforces this conclusion: the free edges of the epidermis do not shorten simply by contraction of individual cells; they zip up by formation of

new contacts between cells that were previously separate. Our dextran-loading experiments show that cells once at the wound margin can later be found lying along the zipped-up seam as the wound closes. How is this process related to the presence of the actin cable? At the two ends of the incisional wound, the cable will pull on the intracellular sides of the cell–cell junctions. Under the resulting force, these actin anchorage points presumably shift along the surfaces of the adherent cells, changing the pattern of contacts so that new pairs of cells are brought into apposition, forming junctions with one another and creating new cable anchorage sites as cells of the original wound margin retire from the marginal row (Fig. 6).

If the actin cable drives the zipping-up of the wound in this way, what happens to the actin that formed the cable segment in a cell that has retired from the wound margin? One attractive suggestion would be that just as the cable is formed in response to the special pattern of stress at the wound edge, so it disassembles as the pattern of stress reverts to that of intact epithelium once the cell has made its exit from the marginal row. Disassembly takes a little while, and consequently, we see a trail of filamentous actin in the recently formed seam formed by the zipping-up process.

In this paper we have given evidence that the small GTPase Rho has a critical role in the healing of a wound in embryonic epidermis: if Rho is inactivated in cells at the wound margin, no actin cable forms in them, and healing fails. Somehow small GTPases such as Rho mediate a link between extracellular signals, such as altered tensile stresses and cytokines, and the machinery of the cytoskeleton and cell–cell adhesion, by which cells change their shape and their attachments in vitro and in vivo. The precise nature of this link stands out as a central problem if we are to understand fully the self-sealing behavior of epithelia in response to damage and, indeed, the events of epithelial morphogenesis in general.

J. Brock and P. Martin thank the Wellcome Trust, and J. Lewis thanks the Imperial Cancer Research Fund for funding these studies. We also thank Catherine Haddon for the artwork in Fig. 6, Dr. Andy Forge for letting us use his SEM, and Dr. Kate Nobes for helping us with the N17rac titration studies in Swiss 3T3 fibroblasts. Finally, we gratefully acknowledge Professor Alan Hall and Dr. Kate Nobes for their critical reading of our paper.

Received for publication 26 February 1996 and in revised form 29 August 1996.

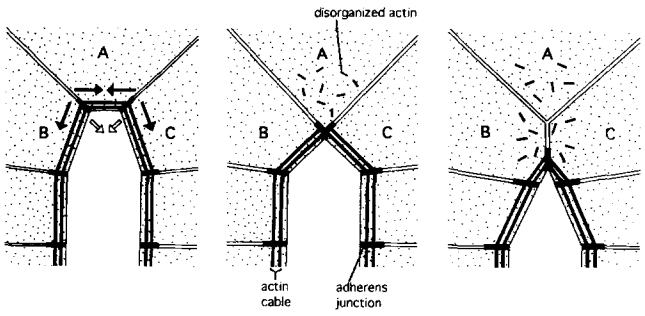

Figure 6. Cartoon to suggest how the epithelium zips up. Three successive stages are shown (*earliest at left*). The cells are linked mechanically by adherens junctions (*short black bars*) that serve as anchorage points for segments of actin cable. Tension in the cable (*solid arrows in lefthand drawing*) creates a centripetal zipping-up force (*hollow arrows*). This causes the adherens junctions to move (either by sliding or by assembly and disassembly) so that eventually cell *A* becomes excluded from the wound margin and cells *B* and *C* become new neighbors. As the junctions move, the actin cable shortens and disassembles, leaving disorganized filamentous actin in its wake.

References

Bement, W.M., P. Forscher, and M.S. Mooseker. 1993. A novel cytoskeletal structure involved in purse-string wound closure and cell polarity maintenance. *J. Cell Biol.* 121:565–578.

Buck, R.C. 1979. Cell migration in repair of mouse corneal epithelium. *Invest. Opthalmol. Visual Sci.* 18:767–784.

Caplan, A.I., and S. Koutroupas. 1973. The control of muscle and cartilage development in the chick limb: the role of differential vascularisation. *J. Embryol. Exp. Morphol.* 29:571–583.

Eaton, S., P. Auvinen, L. Luo, and K. Simons. 1995. Cdc42 and Rac1 control different actin-dependent processes in the *Drosophila* wing disc epithelium. *J. Cell Biol.* 131:151–164.

Grinnell, F. 1992. Wound repair, keratinocyte activation and integrin modulation. *J. Cell Sci.* 101:1–5.

Hall, A. 1994. Small GTP-binding proteins and the regulation of the actin cytoskeleton. *Annu. Rev. Cell Biol.* 10:31–54.

Hamburger, V., and H.L. Hamilton. 1951. A series of normal stages in the development of the chick embryo. *J. Morphol.* 88:49–92.

Harden, H., H.Y. Loh, W. Chia, and L. Lim. 1995. A dominant inhibitory version of the small GTP-binding protein Rac disrupts cytoskeletal structures and inhibits developmental cell shape changes in *Drosophila. Development (Camb.).* 121:903–914.

Hariharan, I.K., K-Q. Hu, H. Asha, A. Quintanilla, R.M. Ezzell, and J. Settleman. 1995. Characterization of rhoGTPase family homologues in *Drosophila melanogaster*: overexpressing Rho1 in retinal cells causes a late developmental defect. *EMBO (Eur. Mol. Biol. Organ.) J.* 14:292–302.

Karnovsky, M.J. 1965. A formaldehyde-gluteraldehyde fixative of high osmolarity for use in electron microscopy. *J. Cell Biol.* 27:137–138.

Kolega, J. 1986. Effects of mechanical tension on protrusive activity and microfilament and intermediate filament organization in an epidermal epithelium moving in culture. *J. Cell Biol.* 102:1400–1411.

Luo, L., Y.J. Liao, L.Y. Jan, and Y.N. Jan. 1994. Distinct morphogenetic functions of similar small GTPases: *Drosophila* Drac1 is involved in axonal outgrowth and myoblast fusion. *Genes & Dev.* 8:1787–1802.

Martin, P., and J. Lewis. 1989. Origins of the neurovascular bundle: interactions between developing nerves and blood vessels in embryonic chick skin. *Int. J. Dev. Biol.* 33:379–387.

Martin, P., and J. Lewis. 1992. Actin cables and epidermal movement in embryonic wound healing. *Nature (Lond.).* 360:179–183.

McCluskey, J., and P. Martin. 1995. Analysis of the tissue movements of embryonic wound healing - DiI studies in the limb bud stage mouse embryo. *Dev. Biol.* 170:102–114.

Nobes, C., and A. Hall. 1995. Rho, Rac, and Cdc42 GTPases regulate the assembly of multimolecular focal complexes associated with actin stress fibers, lamellipodia, and filopodia. *Cell.* 81:53–62.

Odland, G., and R. Ross. 1968. Human wound repair. I. Epidermal regeneration. *J. Cell Biol.* 39:1135–1151.

Paterson, H.F., A.G. Self, M.D. Garrett, I. Just, K. Aktories, and A. Hall. 1990. Microinjection of recombinant p21rho induces rapid changes in cell morphology. *J. Cell Biol.* 111:1001–1007.

Ridley, A.J., and A. Hall. 1992. The small GTP-binding protein rho regulates the assembly of focal adhesions and actin stress fibers in response to growth factors. *Cell.* 70:389–399.

Ridley, A.J., H.F. Paterson, C.L. Johnston, D. Diekmann, and A. Hall. 1992. The small GTP-binding protein Rac regulates growth factor-induced membrane ruffling. *Cell.* 70:401–410.

Ridley, A.J., P.M. Comoglio, and A. Hall. 1995. Regulation of scatter factor/hepatocyte growth factor responses by ras, rac, and rho in MDCK cells. *Mol. Cell. Biol.* 15:1110–1122.

Stenn, K.S., and L. DePalma. 1988. Re-epithelialization. *In* The Molecular and Cellular Biology of Wound Repair. R.A.F. Clark and P.M. Hensen, editors. Plenum Press, New York. 321–335.

Tsukita, S., S. Tsukita, A. Nagafuchi, and S. Yonemura. 1992. Molecular linkage between cadherins and actin filaments in cell-cell adherens junctions. *Curr. Opin. Cell Biol.* 4:834–839.

Wulf, E., A. Deboben, F.A. Bautz, H. Faulstich and T. Wieland. 1979. Fluorescent phallotoxin, a tool for the visualization of cellular actin. *Proc. Natl. Acad. Sci. USA.* 76:4498–4502.

Young, P.E., T.C. Pesacreta, and D.P. Kiehart. 1991. Dynamic changes in the distribution of cytoplasmic myosin during *Drosophila* embryogenesis. *Development (Camb.).* 111:1–14.

Young, P.E., A.M. Richman, A.S. Ketchum, and D.P. Kiehart. 1993. Morphogenesis in *Drosophila* requires nonmuscle myosin heavy chain function. *Genes & Dev.* 7:29–41.